

On-line estimation of circulating fluidized bed boiler fuel composition

Enso Ikonen¹ Markus Neuvonen¹ Istvan Selek¹ Mikko Salo² and Mika Liukkonen²

Abstract—Estimation of power plant fuel input fractions based on unscented Kalman filtering using a first principles simulation model of the furnace is considered. The approach is described, together with experimental results using data from a full scale circulating fluidized bed power plant. The results encourage the fusion of machine learning and physical models in monitoring of industrial processes.

Keywords: biomass, energy production, fouling, machine learning, monitoring, power plants.

I. INTRODUCTION

Circulating fluidized bed (CFB) boilers are largely used for combustion of various fuels in order to produce live steam. Steam is further used for generation of electricity in steam turbines and/or as a source of heat for process industry or district heating. Flexibility in combusted fuel is an important advantage of CFB power plants. Fuel properties have an important impact to plant behaviour and performance.

This study considered fuels such as forest wood chips, demolition wood (chips), combustion peat, and sawdust. While the fuel heat value determines the amount of generated heat, many other fuel characteristics are of importance for process operation and maintenance, emissions, etc.: moisture, particle size and shape, elementary composition of sulfur or nitrogen, alkalines, etc. In many cases the quality and type of fuel vary a lot during normal operation, depending on availability and price of fuels, fuel storages, power and electricity demand and prices, availability of plants in the electricity/heat networks, daily and seasonal weather, etc.

Fouling is the accumulation of unwanted material on solid surfaces. A particular focus of the work was on the impact of fuel characteristics to fouling at heat exchange surfaces between exhaust gases and the water-steam cycle. While fouling on surfaces is a complex process, it is known that both the fuel composition and process operating conditions (temperatures, gas and sand velocities, etc.) do have a significant impact.

Direct measurement of fuel qualities from feed silos or feeding lines is complicated. This is due to harsh conditions at site (dust, moisture, temperatures) and high variety of fuels (composition, particle size, moisture), see Figs. 1–3. Physical installations of the analytics systems require a lot of maintenance (e.g., taking of samplings, cleaning of lenses and lightning, calibration of analyzers), and only a small fraction of the total fuel flow can be analyzed on-line. Moreover, measurement of some fuel properties, such

as alkali content, is difficult and expensive. Therefore it is of interest to consider indirect measurements, at best already existing at the process plant.

Fouling in boilers has been extensively studied, recent papers on model-based monitoring include, e.g., [2][3]. Past



Fig. 1. A typical biomass CFB boiler with fuel storage stockpiles [1].



Fig. 2. Front-end loader and demolition wood [1].



Fig. 3. Wood-based fuel feed fractions [1].

¹Enso Ikonen, Markus Neuvonen and Istvan Selek are with the Intelligent Machines and Systems (IMS) Research Unit, University of Oulu, PL 4300 FIN-90014 Oulun yliopisto, Finland enso.ikonen@oulu.fi

²Mikko Salo and Mika Liukkonen are with the Sumitomo SHI FW Energia Oy, Varkaus, Finland mika.liukkonen@shi-g.com

works on state estimation methods applied to fouling in boilers include [4] who considered constrained unscented Kalman filtering (UKF) and moving horizon estimator in a stirred tank reactor. Monitoring of fuel characteristics in CFB in this connection has been less examined. On-line estimation of fuel moisture and heat transfer coefficients in a circulated fluidized bed boiler was examined in [5], in [6] also air leakage was considered. The current work can be seen as an extension to these, considering the use of state estimation to relate the input fuel characteristics with measurable plant behaviour at later stages in the furnace, flue gases and steam cycle. In the current work, a much more challenging task of detection of fuel input composition with varying fuel types is considered, including testing in a full scale environment as well as implementation aspects. While this paper examines the UKF with a full scale physical model simulations, in [7] subspace identification on the basis of simulated data was used to construct a linear model and methods then developed for the estimation of fuel elementary components.

The remainder of the text is constructed as follows. Section II presents the plant, its model and the available data. Sections III-IV describe the UKF algorithm and its application to fuel composition estimation, to complete the presentation the UKF algorithm is given in the Appendix. Section V illustrates the approach with real data from a full scale power plant. The paper ends with conclusions.

II. PLANT MODEL AND DATA

The considered biofuel plant is a 110 MW_{th} CFB designed for combustion of fuels ranging from forest wood chips to demolition wood, peat and sawdust, situated in the Northern Europe.

A. Physical hotloop model

A physical model for the CFB furnace was available, called *hotloop* model [8][5]. This model is used by the manufacturing company Sumitomo SHI FW Energia Oy for plant design purposes. It describes phenomena related to combustion, fluidization and heat transfer, and covers the entire solid cycle present in a circulating fluidized bed. The model can be considered as detailed in terms of combustion vs. heat generation and fluidization, but less reliable in terms of emission formation. The considered part of the model does not cover the water-steam side processes, nitrogen oxide treatment with ammonia or sulphur-limestone reactions. Also the impact of fuel particle size is not taken into account by the hotloop model.

The hotloop model has been applied at various plants, ranging from small test facilities of few MW to full scale plants of several hundred MW, and has been used to describe both air and oxyfuel combustion ([8][5][9], etc.) The hotloop model available for the research was set up for the 110 MW pilot site design values, but no adjustments with the real plant measurements were conducted before.

The hotloop model inputs consist of fuel feed flows, primary and secondary air flows with compositions and temperatures at various levels of the furnace and return path,

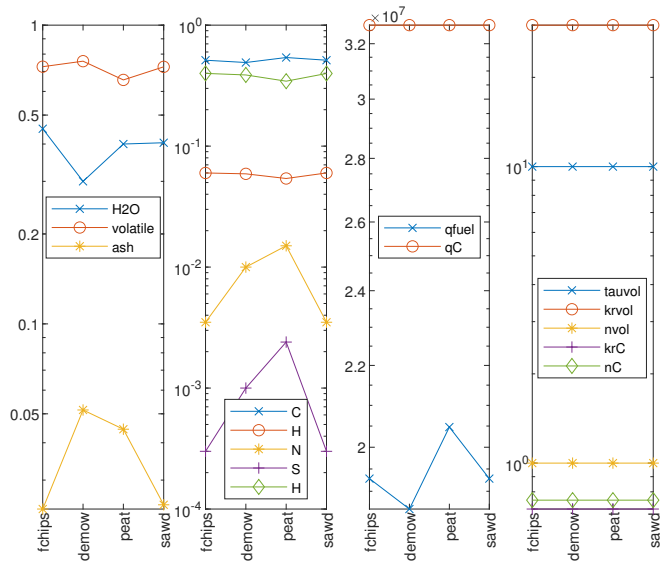


Fig. 4. Hotloop fuel types.

heat transfer surface temperatures, heat transfer coefficients and solids control. There are more than one hundred inputs in total. The dynamic model consists of more than thousand system states. The hotloop model is implemented in MATLAB Simulink, with core parts of the code written as c-code and compiled to mex. The simulink model was executed from the MATLAB workspace using the sim-command. The over one hundred model outputs include predictions of flue gas flow, composition and temperature, heat transfer at various parts of the boiler, furnace temperature and pressure profiles, and estimates of produced power at various sections of the furnace.

The hotloop model defines input fuels as mass feeds of given fuel types [kg/s]. For the 110 MW plant case, four fuel types were specified: forest wood chips, demolition wood, peat and sawdust. The required properties for the fuel types include moisture, volatiles, composition (ash, C, H, N, S, H, summing to unity), heat value of fuel, and char and volatile combustion reaction parameters. Example properties for fuel types are illustrated in Fig. 4. The hotloop inputs include the mass flows for each of the defined fuel fractions.

From Fig. 4 it can be observed that the moisture content of the fuels varies between 30–45 %. Demolition wood is the driest of the fuels, but it also has the highest ash content. It is apparent that peat has the highest upper heat value and sulphur content. The lower heat values are obtained by taking the moisture into account, leading to 13.0 MJ/kg for demolition wood, 12.3 MJ/kg for peat, 11.5 MJ/kg for sawdust and 10.6 MJ/kg for woodchips. It is difficult to distinguish between woodchips and sawdust based on these characteristics. In real life, the particle size distribution of woodchips and sawdust is very different, which impacts fluidization and zones of combustion, but the hotloop model is not able to take that into account. Based on this, and confirmed by experimentation, sawdust was not considered as a fuel type in state estimation.

B. Measurement data

A 17 day dataset from Spring 2014 was available for basic studies. The dataset consisted of a plant start up, followed by fuel tests. The data contained measurements of fuel and air flows, furnace temperatures and pressures, flue gas components (O_2 , SO_2 , NO_x , H_2O , HCl) after furnace and/or from stack, feedwater and steam flows, temperatures and pressures, etc.

The set of plant measurements consisted of more than 200 signal positions, resampled from 5 to 20 second sampling interval for research purposes. The main mechanism for providing a fuel mixture was the operation of the front-end loader filling the fuel conveyer belt from fuel storage piles (cf. 2). No direct measured information about the composition of the fuel fed into the boiler was available. The set of recorded measurements was not complete as many of the data columns contained sections of missing data. The total mass flow of the feed was available for approximately 70% of the test period. The primary air measurements were available. As significant part of air feeds were judged to be missing based on flue gas analysis, the secondary air flows were estimated based on the measured flue gas flow and distributed according to the available measurements. The design operating principle of feeding secondary airs to lower levels at lower production rates was not implemented in simulations. Furnace temperature measurements were available at several levels of the furnace. While the thermocouple measurements provided reliable outcomes, the pyrometer measurements contained a lot of noise. The flue gas emission measurements were partly available only from the stack. In general, the steam side measurements were well available.

C. Tuning of the physical model

With these relatively strong assumptions to compensate for uncertainties in measurements and to close the balances, the data could be used to construct inputs for the hotloop model. A 10 day data set was selected, based on the availability of central measurements (total fuel flow) and apparent stability in production (no major start ups or trippings).

The model was calibrated following the idea of output calibration [10]. For simplicity, only affine static tuning was conducted. Each hotloop output which could be associated with a particular measurement signal or a statistic based on several measurements, was adjusted by finding the bias and gain in an affine transformation, $y_i(k) = ay_{HL,i}(k) + b$, by minimizing the sum of squared deviations from the measurements. The resulting tuned output was then used in model prediction in the state estimation application. Hence, coefficients a close to 1 and b close to zero (in the scale of the signal) indicate that the adjustments made to the hotloop remain relatively small. In the physical model tuning phase, the tuning coefficients for flue gas oxygen resulted in $y_{O_2}(k) = 1.01y_{HL,O_2}(k) + 0.016$ [%/100-mass], i.e., only relatively modest modifications were required. For moisture and flue gas SO_2 , the SSE minimum was obtained with somewhat larger coefficients, reflecting that the model

does not contain a full set of equations governing the SO_2 emission formation and reduction, and SO_2 are only roughly estimated by the hotloop model. For temperatures, the gains varied from 0.3 to 1.3 with associated shift changes of several hundreds of degrees, reflecting that the information obtained of the furnace (and steam) temperature was not exactly corresponding to model components. This is a relatively common problem in combustion plants, as the model predicts the furnace (1D) temperatures, while measurements reside at the side of the plant, and the height of the combustion zones is sensitive to the fuel particle size, among others. With the adjustments in hotloop outputs, the correspondence with measurements could be considered as good, however. The amount of data was not considered sufficient for adjusting the model dynamics with FIR components [10], and the dynamics of the physical model were used in the UKF predictions. This common situation underlines the importance of feasible methods for physical model tuning [10][11].

III. UNSCENTED KALMAN FILTER

Unscented Kalman filter (UKF) [12][13] is an implementation of the bayesian state estimation for the filtering problem. Similar to the Kalman filter (KF) and extended Kalman filter (EKF) [13], or ensemble Kalman filter (EnKF) [14], it uses the signal mean and covariances to describe the uncertainties. This is in contrast to grid-based filtering (GF) [15] or particle filtering (PF) [16], which allow for a much wider class of uncertainty densities to be modelled. The PF and EnKF are based on approximating the distributions by propagating random samples of it, GF relies on finite discretization of the space. While KF uses linear (state space process) models, UKF, EnKF and EKF can handle nonlinear models.

Many practical applications involve heavy simulation models. For example, each model evaluation may require solving the ode equations for one sampling time ahead, which can consume a lot of computation power. In such cases the GF and PF become infeasible in practice, but with EKF, EnKF and UKF the computational load may remain feasible. EKF uses on-line linearization of the nonlinear mappings (via computation of the Jacobians). UKF approximates the distribution using a deterministic sampling (the so called unscented transform). The Jacobians in EKF can also be estimated using finite differences, which makes the approaches quite close. In general, the UKF estimates the propagation of uncertainties in a nonlinear mapping somewhat more precisely than the EKF ([13], Ch. 14.3). There are several versions of the UKF, the choice of which depends on the properties of nonlinearities associated with noise and computational aspects (robustness, speed).

The basic UKF algorithm is well known and given in the Appendix following Simon (Ch 14.3) [13]. In implementation, a scaling parameter W^0 [17] was considered, setting $W^0 = 0$ resulted in the basic form. The basic algorithm assumes that the process and measurement equations are linear with respect to the noise. If this is not a feasible assumption, an approach can be used where noise is augmented onto the state vector, i.e., $x^T \leftarrow [x^T, w^T, v^T]$.

IV. FUEL COMPOSITION ESTIMATION

One potential approach for estimating boiler input fuel composition is to take advantage of the hotloop model and use it in the UKF context. In this approach, the hotloop would provide the state-space model in UKF (f, h) , with inputs u and measurements y coming from the plant. However, some characteristics of the problem complicate a direct application.

- Since the components to estimate would be in the system inputs, the unknown inputs u' need to be added as extended system states $x'^T = [u'^T, x^T]$ in the UKF formulation.
- The pilot hotloop model consists of more than a thousand states. This is too much to estimate in a practical implementation due to the computational burden in simulating the physical model. Hence, a selection must be made and only a subset x'' of states x' considered uncertain in the UKF context. In an extreme case $x'' = u'$ can be taken, and the propagation of the remaining states predicted using the plant model f .
- The total fuel feed was measured from the pilot plant. The total estimated feed is the sum of the feeds of fuels of different types. A prediction of the total feed can be constructed by summing the estimated feeds.
- The set of UKF measurements was chosen to be the measured flue gas composition: H_2O , O_2 , SO_2 ; furnace temperatures at the bottom, 9.6 m and exit (separator), and total fuel flow. The states to be estimated were chosen as the minimal set, including only the unknown fuel feeds of three possible types.
- Due to tuning, the UKF innovation signal was constructed by inverting the measurement with the tuning parameters $z_i = \frac{1}{a_i} (y_i(k) - b_i)$ and comparing z_i signal with the hotloop prediction $y_{HL,i}(k)$. The estimates for the measurement covariances were scaled accordingly by multiplying with $1/a_i^2$.

V. EXPERIMENTAL

A set of simulation experiments was conducted on a 10 day data from the 110 MW plant. The test period included experimental verification tests on fuel performance for the pilot plant, conducted at the end of the commissioning phase.

The UKF estimate was constructed by choosing the output variables measured from the plant and predicted by the tuned hotloop model. The measurements (flue gas oxygen, sulphur, moisture and temperatures from the bottom, middle and top of the furnace) were selected after some experimentation. In addition, the total amount of fuel feed was measured. The UKF relies on knowledge on the state and measurement uncertainties, i.e., noise distributions are assumed to be zero mean with covariances \mathbf{Q} and \mathbf{R} . The measurement uncertainties $\mathbf{R}(k)$ were chosen as squares of the approximate effective scale of the used variables: $5 \times 0.15/100$ for H_2O , $0.04/100$ for O_2 , $10 \times 0.0002/100$ for SO_2 , $500/100$ for temperatures and $0.2 \times 10/100$ for the total fuel feed, where the coefficient ($C \times$) reflects tuning. The state uncertainties were chosen as $\mathbf{Q}(k) = 0.01 \times \sqrt{0.02^2} \mathbf{I}$, with initial uncertainties $\mathbf{P}(0) = 0.1 \times 0.5^2 \mathbf{I}$.

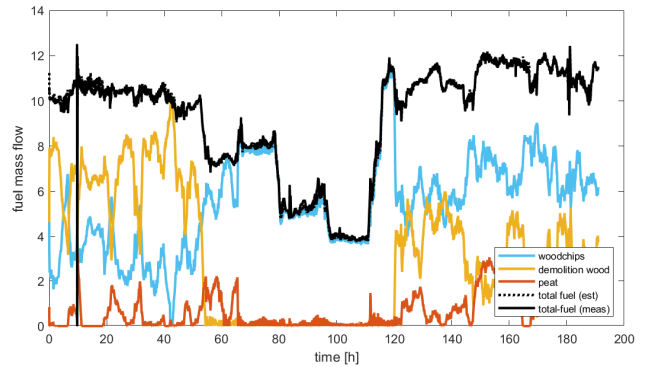


Fig. 5. Fuel monitoring with fuel types: woodchips, demolition wood and peat.

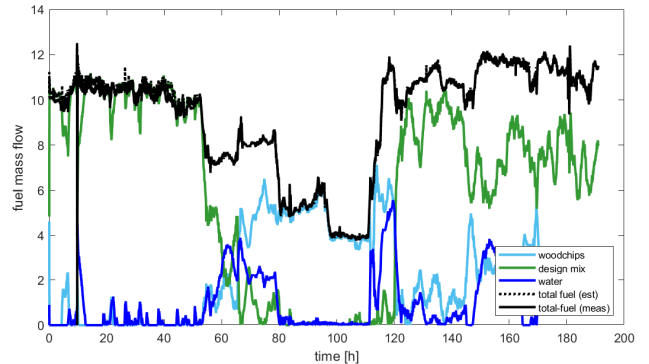


Fig. 6. Fuel monitoring with fuel types: woodchips, design mixture and water (fuel moisture).

Figure 5 illustrates the outcomes of the hotloop/UKF fuel quality estimation. The UKF estimated the fractions of three potential fuels: woodchips, demolition wood and peat, with respective physical properties defined in the hotloop model fuel palette. The data contains intervals of some hours with a known fuel composition, namely: two runs at 100 % load with design mixture of peat, demolition wood and woodchips, one run at 70 % load with design mixture, 40 % load with wood chips only, and 30 % load with wood chips. These intervals occur approx. at 12, 36 and 60 hours for the mixture tests, and 84 and 108 hours for the woodchips, respectively. For the mixture tests, the small amount of peat is correctly estimated, as well as that there are larger fractions of demolition wood and woodchips. The internal fractions of wood are not correct, however, as the estimate suggests a larger fraction of demolition wood than that of woodchips, which was not the case. The fuel fractions at lower power levels are correctly estimated as 100 % woodchips. The estimates at other time intervals can be assessed as plausible, even if no full knowledge of fuel during these intervals was available.

In another setup, the fuel fractions were defined as default mixture, woodchips and moisture. Figure 6 illustrates the estimation with this setup. At 100 % power level, the fuel is correctly estimated as the mixture, at 70 % the estimate

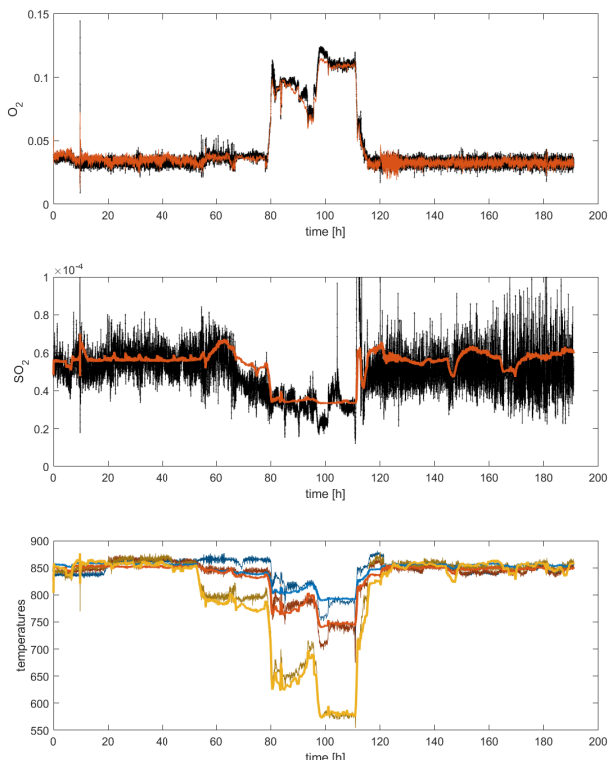


Fig. 7. Predictions vs. measurements. Tuned posterior predictions, $y_{HL} = h(\hat{x}^+)$ (see Appendix for notation), $\hat{y}_i = a_i y_{HL,i} + b_i$ are shown. Top plot: O_2 , middle plot SO_2 , bottom plot: furnace temperatures. Measured signals are shown in darker colors.

proposes not only a reduction in fuel feed but also increase of moisture. At lower power levels, the fuel feed is again correctly estimated to consist of woodchips. Again, the estimates at other time intervals can be assessed as feasible.

Figure 7 illustrates some of the measurements and the corresponding predictions by the UKF. The UKF innovation signal is constructed by inverting the affine tuning components and comparing the signal with the corresponding hotloop prediction. Fig. 7 shows the tuned a posteriori predictions with the plant measurements. It is clear that the oxygen and sulphur in flue gases, as well as the furnace temperature profile, have a significant impact on the estimate.

The desired outcome of the fuel composition estimation is the flow of elementary components to the boiler. It is straightforward to construct the composition (ash, C, H, N, S, H) of the feed by multiplying the estimated feed rates by the respective compositions. Figure 8 illustrates the elementary composition of the fuel, as derived from the estimated fuel fractions and their characteristics. This information is expected to be useful in further work on monitoring of the heat exchange surface fouling.

A significant obstacle in simulation studies was due to the time taken by the simulations. With the UKF, $2n + 1$ simulations need to be conducted at each sampling time. On a standard 2020 up-to-date i7 laptop PC, a simulation of 20 seconds of boiler operation took approximately 1 seconds to complete. Hence, simulation of fuel estimation on the 10 day

data set took several days to accomplish. Most of the time is spent with solving the physical model ode's. However, the on-line implementation with a small number of uncertain states (i.e., three fuel fractions) was feasible even with a computing power provided by a standard laptop. A potential alternative for a more significant number of uncertain states could be the examination of the EnKF [14] in the present context.

VI. CONCLUSIONS

This paper considered application of bayesian model-based state estimation using physical model simulations. The work illustrates how conclusions can be drawn on fuel input characteristics with the help of advanced plant models, under the impact of state and measurement noise and plant-model mismatch. The approach was demonstrated in estimating on-line the unknown fuel fractions entering a full scale circulating fluidized bed boiler, using real plant data and a dynamic physical model developed for plant design purposes. As the model consisted of more than thousand state ode's, a UKF with a heavily reduced set of uncertain states was found to perform in a reasonable manner. In a wider perspective, the work targets the generalization of the pilot-driven experiences of estimation of process input characteristics for use in the heavy process industry. The paper emphasizes the largely unused potential of fusion of machine learning [18][19] and physical models [20] in monitoring of industrial processes.

ACKNOWLEDGMENT

This work was conducted in the H2020 project COGNITWIN (grant number 870130).

REFERENCES

- [1] Sumitomo SHI FW Energia Oy. Sumitomo internal image bank, 2021.
- [2] L. Xu, Y. Huang, J. Yue, L. Dong, L. Liy, J. zha, M. Yu, B. Chen, C. Zhu and H. Liu. Improvement of slagging monitoring and soot-blowing of waterwall in a 650MWe coal-fired utility boiler. Journal of the Energy Institute, vol. 96, 106–120, 2021.
- [3] L. Pattanayak, S. Ayyagari and J. Sahu. Optimization of sootblowing frequency to improve voiler performance and reduce combustion pollution. Clean Technolgies & Environmental Policy, vol. 17, 1897–1906, 2015.

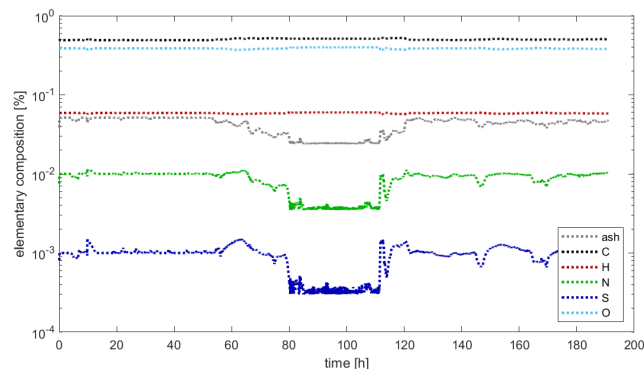


Fig. 8. Estimated elementary composition of fuel.

- [4] B. J. Spivey, J. Hendegren, and T. Edgar. Constrained nonlinear estimation for industrial process fouling. *Industrial and Engineering Chemistry Research*, vol. 49, pp. 7824–7831, 2010.
- [5] E. Ikonen, J. Kovacs and J. Ritvanen. Circulating fluidized bed hot-loop analysis, tuning and state-estimation using particle filtering. *International Journal of Innovative Computing, Information and Control*, vol. 9, nro 8, 3357–3376, 2013.
- [6] M. Hultgren, E. Ikonen and J. Kovacs. Circulating fluidized bed boiler state estimation with an unscented Kalman filter tool. 2014 IEEE Conference on Control Applications, Antibes/Nice, France, 2014.
- [7] M. Neuvonen, I. Selek and E. Ikonen. Estimating Fuel Characteristics from Simulated Circulating Fluidized Bed Furnace Data. 9th International Conference on Systems and Control, Caen, France, 2021.
- [8] J. Ritvanen, J. Kovacs, M. Salo, M. Hultgren, A. Tourunen and T. Hyppänen. 1-D dynamic simulation study of oxygen fired coal combustion at pilot scale CFB boiler. The 21st International Conference on Fluidized Bed Combustion, Naples, Italy, 2012.
- [9] L. Niva, E. Ikonen and J. Kovacs. Self-optimizing control structure design in oxy-fuel circulating fluidized bed combustion. *International Journal of Greenhouse Gas Control*, vol. 43, Dec., 93–107, 2015.
- [10] E. Ikonen and I. Selek. Fusing physical models with measurement data using FIR calibration. *Control Engineering and Applied Informatics*, vol. 23, nro 2, 68–77, 2021.
- [11] T. Bikmukhametov and J. Jäschke. Combining machine learning and process engineering physics towards enhanced accuracy and explainability of data-driven models. *Computers and Chemical Engineering*, vol. 138, 1–27, 2020.
- [12] S. Julier, J. Uhlmann, and H. Durrant-Whyte. A new approach for filtering nonlinear systems. *American Control Conference*, 1620–1632, 1995.
- [13] D. Simon. *Optimal State Estimation - Kalman, Hinf and nonlinear approaches*. John Wiley, 2006.
- [14] M. Katzfuss, J. Stroud, and C. Wikle. Understanding the Ensemble Kalman filter. *The American Statistician*, vol. 70, 350–357, 2016.
- [15] E. Ikonen, I. Selek and K. Najim. Process control using finite Markov chains with iterative clustering. *Computers and Chemical Engineering*, vol. 93, 293–308, 2016.
- [16] N. Gordon, D. Salmond, and A. Smith. Novel approach to nonlinear/non-Gaussian Bayesian state estimation. *IEEE Proceedings-F*, vol. 140, no 2, 07–113, 1993.
- [17] G. Terejanu. Unscented Kalman filter tutorial. Technical report, University of Buffalo <https://www.cse.sc.edu/terejanu/files/tutorialUKF.pdf>, 2011.
- [18] T. Hastie, R. Tibshirani, and J. Friedman. *The elements of statistical learning - Data mining, inference and prediction*. 2nd ed, Springer, 2017.
- [19] S. J. Qin and L. H. Chiang. Advances and opportunities in machine learning for process data analytics. *Computers and Chemical Engineering*, vol. 126, 465–473, 2019.
- [20] S. Skogestad. *Chemical and Energy Process Engineering*. CRC Press, 2009.

APPENDIX

Suppose a n -state discrete-time nonlinear system with state equation

$$x(k+1) = f(x(k), u(k)) + w(k)$$

and a measurement equation

$$y(k) = h(x(k)) + v(k)$$

and assume that state and measurement noises are known to be distributed according to $w(k) \sim (0, Q(k))$ and $v(k) \sim (0, R(k))$. Functions f and h , system inputs u and measurements y , as well as covariances Q and R are known. The UKF is initialized by giving the initial apriori estimates of the state mean and covariance $x^+(0)$ and $P^+(0)$.

(a) Choose $2n$ sigma points in the vicinity of the current guess of state:

$$\hat{x}^{(i)}(k-1) = x^+(k-1) + \tilde{x}^{(i)}$$

where $\tilde{x}^{(i)} = \left(\sqrt{nP^+(k-1)}\right)_i^T$ for $i = 1, 2, \dots, n$ and $\tilde{x}^{(i)} = -\left(\sqrt{nP^+(k-1)}\right)_i^T$ for $i = n+1, \dots, 2n$. In this notation, the \sqrt{nP} is the matrix square root of nP such that $\sqrt{nP}^T \sqrt{nP} = nP$, and \sqrt{nP}_i is the i th row of \sqrt{nP} (see [13]).

(b) Use the system state equation f to propagate the sigma points

$$\hat{x}^{(i)}(k) = f\left(\hat{x}^{(i)}(k-1), u(k)\right)$$

Notice, that $2n$ evaluations of the system dynamics are required, i.e., the system equations in f need to be solved $2n$ times from $t = k-1$ to $t = k$, starting from different initial states, $\hat{x}^{(i)}(k-1)$.

(c)-(d) Combine an apriori state estimate at time k with mean and covariance

$$\hat{x}^-(k) = \frac{1}{2n} \sum_{i=1}^{2n} \hat{x}^{(i)}(k)$$

$$P^-(k-1) = \frac{1}{2n} \sum_{i=1}^{2n} \left(\hat{x}^{(i)}(k) - \hat{x}^-(k)\right) \left(\dots\right)^T + Q(k-1)$$

(e) Use the measurement equation h to predict measurements

$$\hat{y}^{(i)}(k) = h\left(\hat{x}^{(i)}(k)\right)$$

Note that another unscented transform could be used here, based on $P^-(k)$. However, reusing the sigma points from the previous step (based on $P^+(k-1)$) will save some computational efforts.

(f)-(g) Combine the predictions to obtain an estimate with mean and covariance

$$\hat{y}(k) = \frac{1}{2n} \sum_{i=1}^{2n} \hat{y}^{(i)}(k)$$

$$P_y(k) = \frac{1}{2n} \sum_{i=1}^{2n} \left(\hat{y}^{(i)}(k) - \hat{y}(k)\right) \left(\dots\right)^T + R(k)$$

(h) Estimate the cross covariance between x^- and y

$$P_{xy}(k) = \frac{1}{2n} \sum_{i=1}^{2n} \left(\hat{x}^{(i)}(k) - \hat{x}^-(k)\right) \left(\hat{y}^{(i)}(k) - \hat{y}(k)\right)^T$$

(i) The update of the state estimate can now be performed using the Kalman filter equations

$$K(k) = P_{xy}(k) [P_y(k)]^{-1}$$

$$\hat{x}^+(k) = \hat{x}^-(k) + K(k) (y(k) - \hat{y}(k))$$

$$P^+(k) = P^-(k) - K(k) P_y(k) K(k)^T.$$